PHYSICS AND TECHNIQUE
OF ACCELERATORS

Developing an Interferometric Method for Measuring the Transverse Dimensions of a Particle Beam in Cyclic Accelerators

V. L. Dorokhov[a, c, *], O. I. Meshkov[a, b], A. I. Styrin[d], and A. S. Smygachev[a, d]

[a] Budker Institute of Nuclear Physics, Siberian Branch, Russian Academy of Sciences, Novosibirsk, Russia
[b] Novosibirsk State University, Novosibirsk, 630090 Russia
[c] Synchrotron Radiation Facility Siberian Circular Photon Source SKIF Boreskov Institute of Catalysis of Siberian Branch of the Russian Academy of Sciences, Koltsovo, Russia
[d] National Research Center Kurchatov Institute, Moscow, 123182 Russia
*e-mail: V.L.Dorokhov@inp.nsk.su

Abstract—This work is devoted to the development of a method for measuring beam sizes in cyclic charged particle accelerators using an interferometer based on the Young scheme with a double-slit diaphragm. We have carried out an experimental verification of the original spectral method for scanning the interference pattern. The results of measurements of the spectrum of low-frequency oscillations of the beam of the storage ring of the Kurchatov Synchrotron Radiation Source (KSRS) obtained by means of the Optical Observation Station (OOS) of the storage ring are presented.

INTRODUCTION

Modern sources of synchrotron radiation (SR) of the 4th generation [1], which have an ultralow (less than 1 nm) emittance require a high stability of the electron beam to realize the advantages of high brightness and coherence of SR. At the same time, all plant components are inevitably affected by natural, industrial, and domestic vibration sources, with each vibration source having a unique range of frequencies and amplitudes. This contributes to the instability of the position and/or angle relative to the orbital plane of the electron beam and SR, the average value of which should not exceed 10% on the rms beam size and/or the angular divergence of the radiation [2, 3]

In addition to the negative effect on the SR characteristics, the instability of the position of the particle beam can lead to an overestimation of its transverse dimensions, which are determined by the means of optical diagnostics of the setup. Such errors are unacceptable in precision measurements of the beam emittance, which is one of the main characteristics of modern storage rings.

The transverse dimensions of the particle beam density distribution of modern sources of synchrotron radiation are less than 10 μm, and the method of direct imaging in the optical part of the SR spectrum has long been unsuitable for observing such quantities. The simplest and most accessible way to determine the dimensions of the transverse charge distribution in the beam, especially during the commissioning of a new SR source, is double-slit interferometry [4, 5]. The spatial resolution of this diagnostic method, demonstrated on a number of installations, is about 1 μm. Such a profilometer is currently operating at the OOS station [6, 7] of the Kurchatov Synchrotron Radiation Source [8], where the typical measurable value of the vertical beam size at the emitting point used to output the light is ≈ 60 μm.

In the Siberian Circular Photon Source "SKIF", which is currently under construction in the science city of Koltsovo, Novosibirsk area, the characteristic size of the vertical distribution of beam particles at the radiation point used for optical diagnostics, according to calculations, will vary from 8.6 to 28.9 μm, depending on the operating mode of the installation. To obtain the calculated values of the vertical emittance and beam size, in addition to precise methods of tuning the optics, diagnostics will also be required to ensure the possibility of measuring the required values. Therefore, it was proposed to carry out a series of measurements on the SR source at the KSRS to verify the ideas that are supposed to be implemented on the SKIF.

DOUBLE SLIT INTERFEROMETER

Interferometry, as an optical method for measuring small angular dimensions, has long been a generally accepted diagnostic tool in accelerator physics. At the KEK Photon Factory (Japan), this method was first implemented to observe the transverse charge distribution of an electron beam with a size on the order of 10 μm [4, 5]. As a rule, interferometers with wavefront fission are used for beam diagnostics, which operate
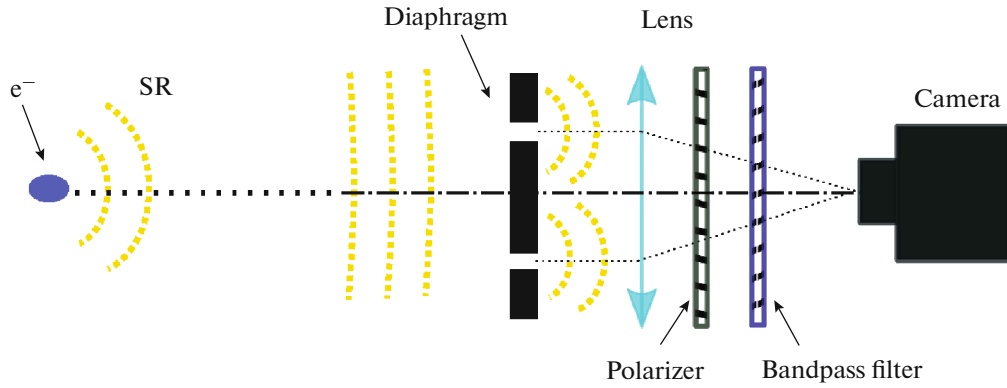
Fig. 1. Two-beam Young interferometer.

with visible polarized quasi-monochromatic SR from the dipole magnet of the setup. The classical scheme of a double-slit Young interferometer is shown in Fig. 1.

The distribution of the intensity of the interferogram obtained using a diaphragm with two elongated slits in the absence of an imbalance in the intensities of light passing through the slits is determined by the expression

$$I(y) = 2I_0 \left(\frac{\sin \alpha}{\alpha}\right)^2 \left[1 + |\gamma_{coh}| \cos\left(k \frac{D}{R} y + \varphi_0(x)\right)\right],$$

$$\alpha = k \frac{a}{2R} y,$$
(1)

where I_0 is the total intensity of radiation passing through the interferometer slit, $k = \frac{2\pi}{\lambda}$ is the wave number, $|\gamma_{coh}|$ is the degree of spatial coherence, $\varphi_0(x)$ is the spatial phase of the interferogram, L is the distance from the radiation source to the diaphragm with slots, a is the slot width, D is the distance between slots, and R is the distance to the interferogram plane.

$$\gamma_{coh} = \int f(x) \exp(-i2\pi\nu x) dx, \quad \nu = \frac{D}{\lambda L},$$
(2)

where ν is the spatial frequency, D is the distance between slots, and L is the distance from the source to the diaphragm. The RMS size of beam intensity distribution σ through $|\gamma_{coh}|$ is expressed as

$$\sigma = \frac{1}{\pi\nu} \sqrt{\frac{1}{2} \ln\left(\frac{1}{|\gamma_{coh}|}\right)}.$$
(3)

The dependence of the accuracy of the calculated beam size on the value of the degree of spatial coherence and the error of its determination follows from (3):

$$\Delta\sigma = \frac{\lambda L}{\pi D} \frac{1}{\gamma_{coh}\sqrt{8 \ln \gamma_{coh}^{-1}}} \Delta\gamma_{coh},$$
(4)

where $\Delta\gamma$ is the error in determining the degree of spatial coherence from the interference pattern. The minimum of this dependence is reached at

$$|\gamma_{coh}| = \exp(-0.5) \approx 0.61.$$
(5)

In Fig. 2 there are curves demonstrating the behavior of dependencies (3), (4). For the interference pattern described by expression (1), the modulus of the degree of spatial coherence is equal to the visibility, defined as

$$V = \frac{I_{max} - I_{min}}{I_{max} + I_{min}},$$
(6)

where I_{max} and I_{min} are the value of the signal at the maximum and minimum of the interference pattern, respectively. By analyzing the image of the interference pattern recorded by a digital camera, it is easy to calculate the size of the radiation source.

During the observation of the beam size in the normal operating mode of the accelerator, a fixed distance D_{opt} between the slits is used, which provides the visibility of the interference pattern close to the minimum of the error function (Fig. 2). From the point of view of the practical implementation of the method, it is desirable to locate the slits at a level close to the maximum of the angular distribution of SR, which ensures the maximum light intensity on the matrix of the recording device. For an example, in Fig. 3, the vertical angular distribution of radiation over the diaphragm of the OOS KSRS interferometer is shown. An increase in the distance between the slits leads to a decrease in the light flux and, accordingly, to the need to increase the exposure time of the recording camera. Distance reduction D is accompanied by a deterioration in the accuracy of measuring the beam dimensions at a fixed wavelength λ (expressions (4), (2), Fig. 2). Thus, it is of importance to maintain the visibility value while not increasing the distance between slits. We propose to vary the spatial frequency ν by changing the central wavelength λ set by the band-pass filter (Fig. 1) while not alternating the distance D_{opt} during regular calibrations, diagnostics, and accelerator physics experiments, when the beam emittance changes. In addition, this will make it possible to make the design of the light splitting unit simpler for the concurrent observation of the vertical and horizontal dimensions of the particle beam by two independent interferometers with a slit diaphragm.
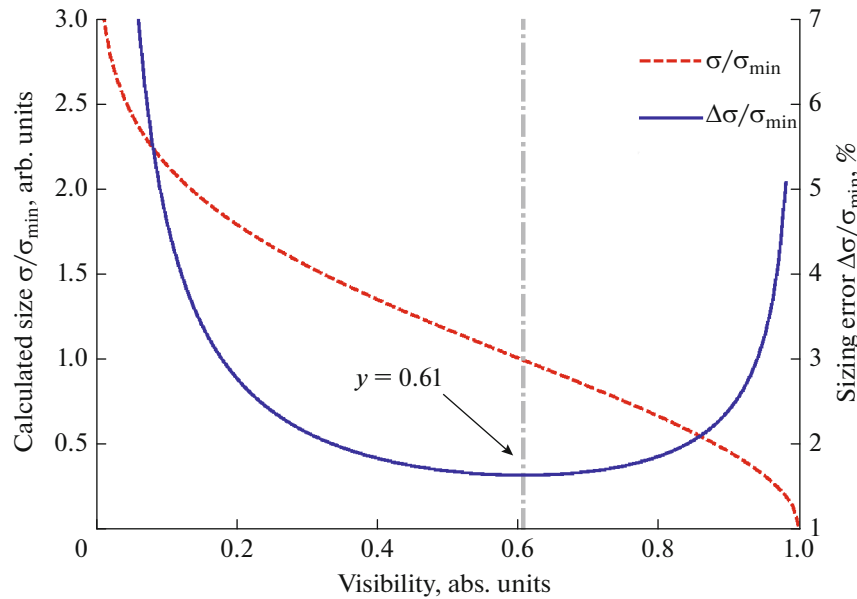
Fig. 2. Dependences of the beam size and its error on visibility. The error in determining the visibility of the interference pattern ($\Delta\gamma_{coh}$) is taken equal to 1%. Both dependences are normalized to the beam size at $\gamma = 0.61$ (σ_{min}).

DESCRIPTION OF INSTALLATION

The 3D model of the optical observation station is shown in Fig. 4. The elements of optical diagnostics of the beam are located on the optical table, which is mounted on a steel frame attached to the floor of the experimental hall and the bioprotection wall.

The OOS station receives light from the bending magnet of the superperiod of the KSRS storage ring (Fig. 5). At the point of the orbit from which synchrotron radiation is output to OOS, the calculated optical functions are: $\beta_x = 1.936\,\mathrm{m}$, $\eta_x = 0.377\,\mathrm{m}$, and $\beta_y = 6.529\,\mathrm{m}$.
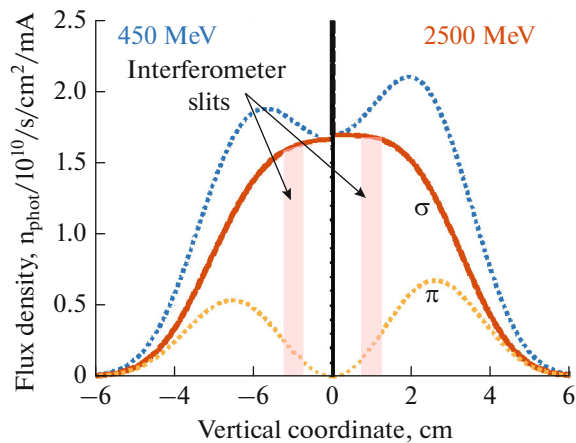
Fig. 3. Vertical distribution of the SR photon flux on the slit diaphragm of the interferometer for injection and experiment energies; σ component and π component and total flux density.

The vertical beam size in the KSRS storage ring is close to the diffraction limit in the optical wavelength range. For this reason, a double-slit interferometer is used at the OOS station for its correct measurement [7]. Along with interferometric measurements, the traditional projection method of recording a beam image with a digital camera is also used. In addition, the OOS includes four more detectors, which forces the use of a large number of optical elements to divide light between them. For simplicity, in Fig. 6, the scheme of light division only between the interferometer and the camera, which records the optical image of the particle beam, is presented. The interferometer uses a small part of the SR incident on the first optical diagnostic mirror, which significantly limits the minimum exposure time of its digital camera. In our measurements, to increase the amount of light falling on the camera matrix, all other OOS detectors were excluded from the optical scheme (see Fig. 6), and images were recorded with a Daheng MER-131-75GM digital camera. Unlike Prosilica GC1290, which is used regularly at the OOS station, it allows one to confidently read frames with a frequency of up to 2.3 kHz using specially designed software. This scheme was easily transformed into an interferometer by installing a diaphragm with slits in front of the lens. In the method of spectral scanning of interefrence pattern,. four band-pass filters were used with a full width at half maximum $\Delta\lambda = 10\,\mathrm{nm}$. The band-pass filters of the interferrometer varied in the range 400−550 nm; the spectral characteristics of the filter pass band and dependences of the quantum efficiency of the Daheng MER-131-75GM camera are shown in Fig. 8.
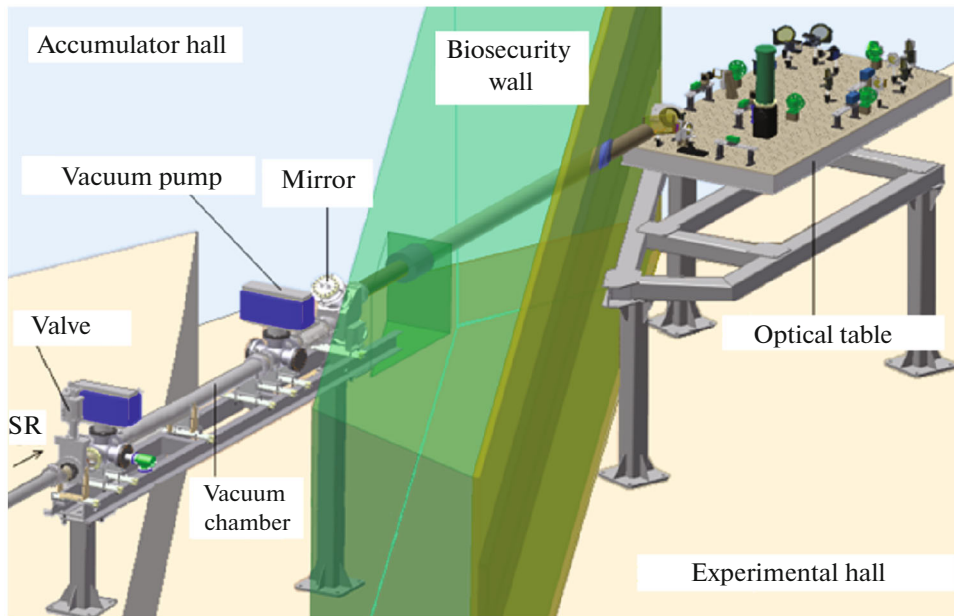
Fig. 4. 3D model of the diagnostic station. The vacuum channel for the SR output from the bending magnet is visible.
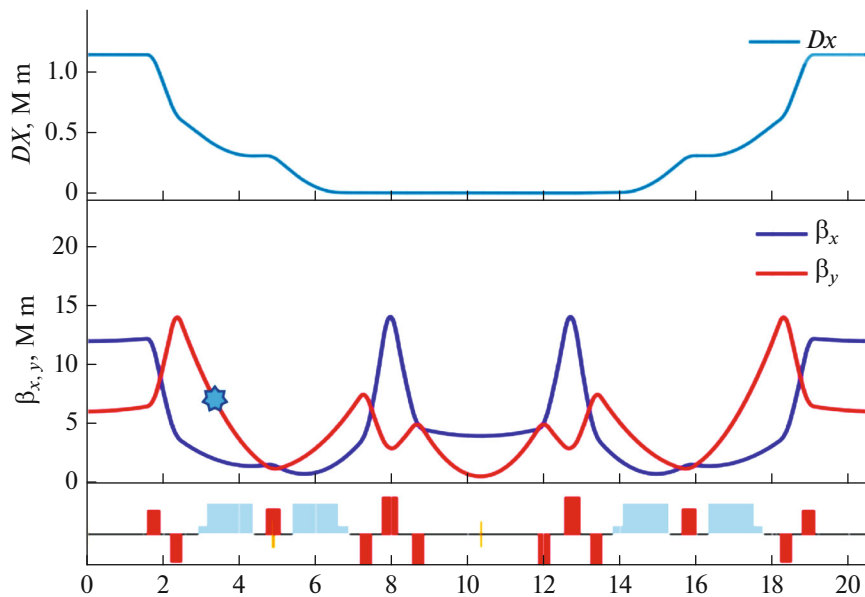

Fig. 5. Optical functions of the main storage ring of the KSRS over the length of the superperiod. The asterisk indicates the location of the light output for OOS.

VIBRATION CHARACTERISTICS OF THE OPTICAL TABLE AND THE VISIBLE CENTER OF MASS OF THE PARTICLE BEAM IN THE STORAGE RING

Previously, it was necessary to find out the vibrational characteristics of the optical table on which the optical diagnostics is located. The point is that the light flux entering the interferometer is limited not only by the bandpass filter and the size of the slots, but also by the aperture of the first mirror installed in front of the main optical objective of the station. In this regard, the exposure time of a digital camera that records the interference pattern has to be increased to several tens of milliseconds or more, depending on the beam current in the storage ring; therefore, transverse beam oscillations with a frequency of tens of milliseconds can lead to a deterioration in the visibility of the interference pattern, i.e., an overestimation of the real vertical size of the beam. This can become a measurement problem for the KSRS, since the comparison of the calculated and experimental beam emittance is
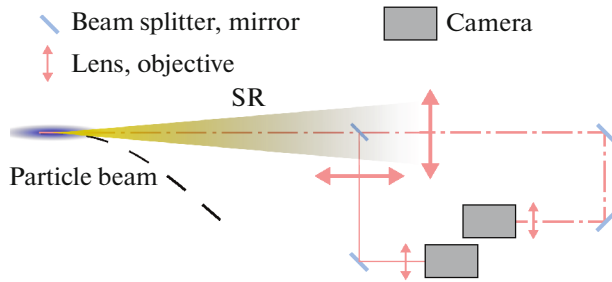
Fig. 6. Scheme of light division between the interferometer and the camera that registers the optical image of the particle beam in the standard OOS configuration.
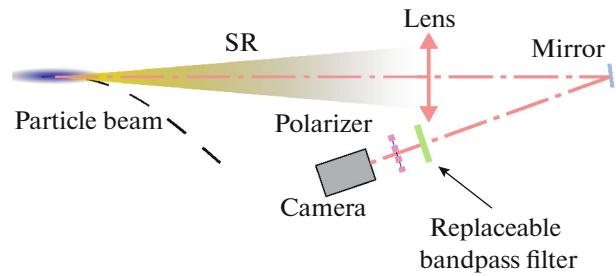

Fig. 7. Scheme of the configuration of the recording optics used in the measurements.
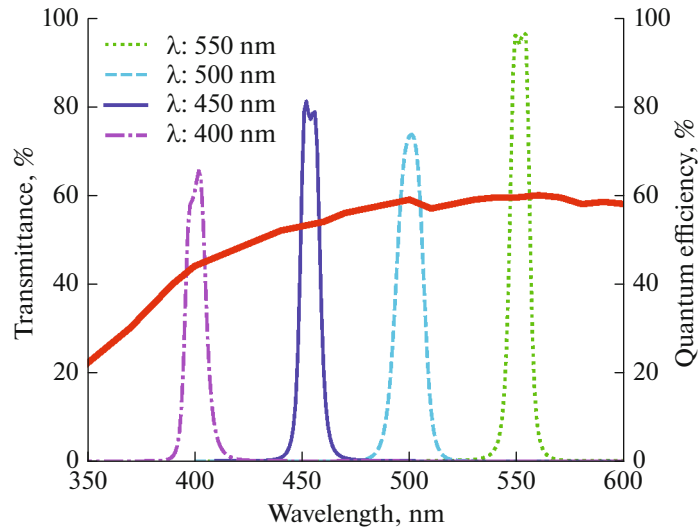

Fig. 8. Spectral transmission characteristics of filters and the dependence of the quantum efficiency of the Daheng MER-131-75GM camera matrix (thick solid curve).

carried out at a minimum number of particles in the bunch to neglect collective effects. The associated proportional decrease in the number of photons emitted by the beam makes it necessary to increase the exposure time of the camera; i.e., getting rid of one problem makes it likely to come up against another, which emphasizes the relevance of our experiments. Generally speaking, the oscillation spectrum of the optical table is certified by the manufacturer, but it needs additional research for a specific mounting method.

Of course, low-frequency transverse oscillations of the beam in orbit, associated, for example, with corrector noise, can also cause systematic errors in measurements of its dimensions. Effects of this kind were occasionally observed by KSRS operators, and the purpose of the experiments was also to elucidate the spectrum of these oscillations.

Vibration characteristics of the table were measured by recording the image of the reference source by a digital camera. As a test object for registration, a laser beam spot projected onto the wall of the facility radiation protection near the optical table of the sta-

tion was used. The camera exposure time was 10 μs. Fourier analysis of the vertical vibrations of the image gravity center (Fig. 9) revealed a maximum with an amplitude of about 3 μm at a frequency of 100 Hz. No noticeable features in the spectrum of horizontal vibrations of the table have not been observed.

Studies of the vertical and radial jitter of the center of mass of the particle beam were carried out using the same technique and software as the measurements of the oscillation spectrum of the optical table. The registered spectrum of fluctuations of the center of gravity of the beam contains a distinct maximum with an amplitude 9 μm at a frequency of 50 Hz and a weak peak with negligible amplitude at the frequency 100 Hz (Fig. 10).

At the same time, the experiments revealed the existence of irregular beam displacements with frequencies less than 1 Hz and scale amplitudes σ_y, whose nature is still unclear. No features above the noise level were recorded in the spectrum of radial beam oscillations. The search for the cause of beam oscillations with a frequency of 50 Hz requires separate investigations.
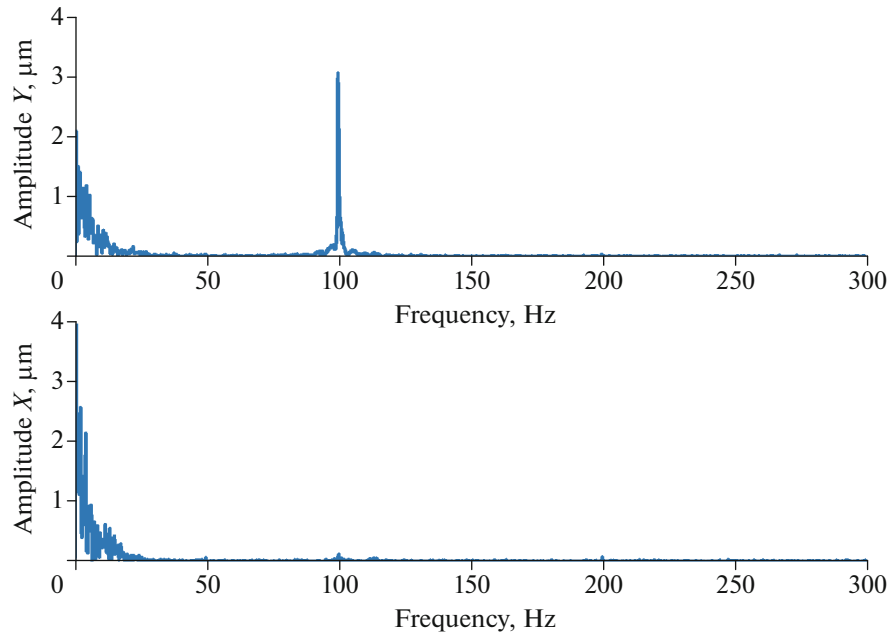
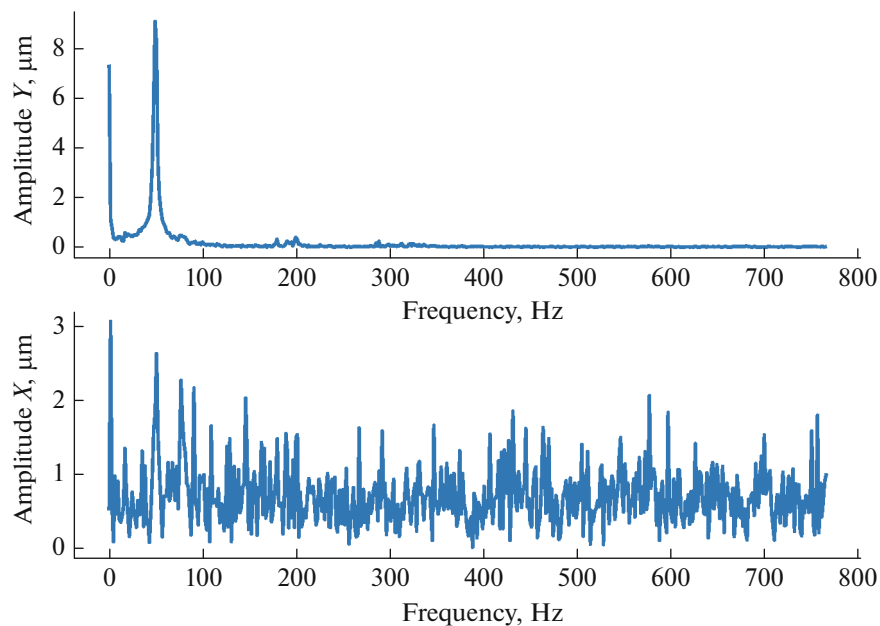**Fig. 9.** Spectrum of oscillations of the optical table of the OOS station.

Fig. 10. Spectrum of fluctuations of the center of gravity of the beam recorded at the OOS station.

VERTICAL BEAM SIZE MEASUREMENTS

In these measurements, the spatial frequency ν changed as a tuning of the wavelength of the registered quasi-monochromatic light λ, given by the band-pass filter, and the distance D between the slits in the diaphragm of the interferometer. For each of the filters, interferograms were recorded with a change in the distance between the interferometer slits within 10—25 mm. The results are presented in Figs. 11—15. The interferograms during the transition from the wavelength of light to 400 nm to the wavelength 550 nm can be compared using Fig. 11; solid curves correspond to the result of approximation of the experimental points by the theoretical dependence (1). As expected, an increase in the wavelength results in an increase in visibility (enhanced contrast) of the intereference pattern and an increase in the distance between interference maxima. Figure 12 shows the increase in visibility when spatial frequency is scanned by changing wavelength for various distances between the slits. The obtained experimental data agree well with the theoretical curve. Figure 13 shows the calculated and mea-
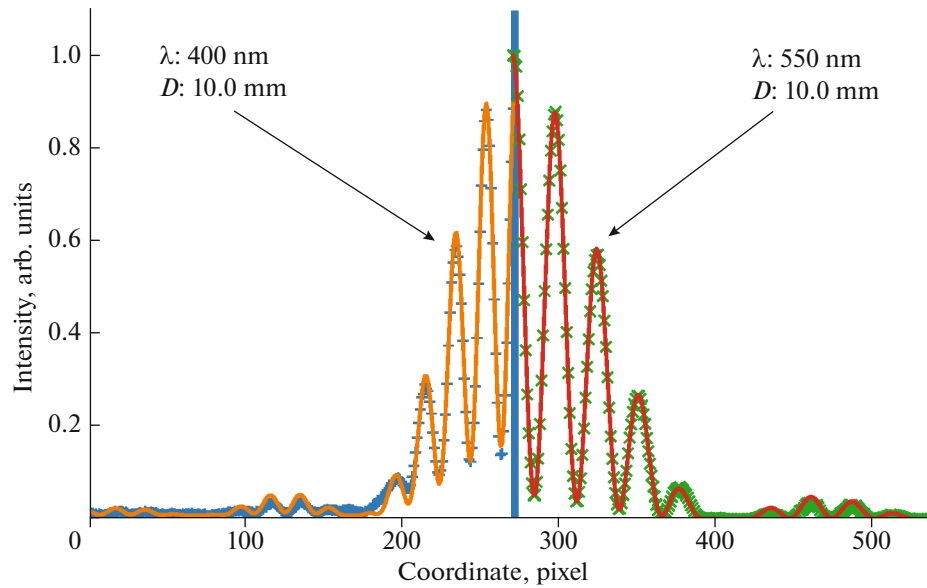
Fig 11. Comparison of recorded interferogram profiles for a diaphragm with the distance between slits $D = 10$ mm.
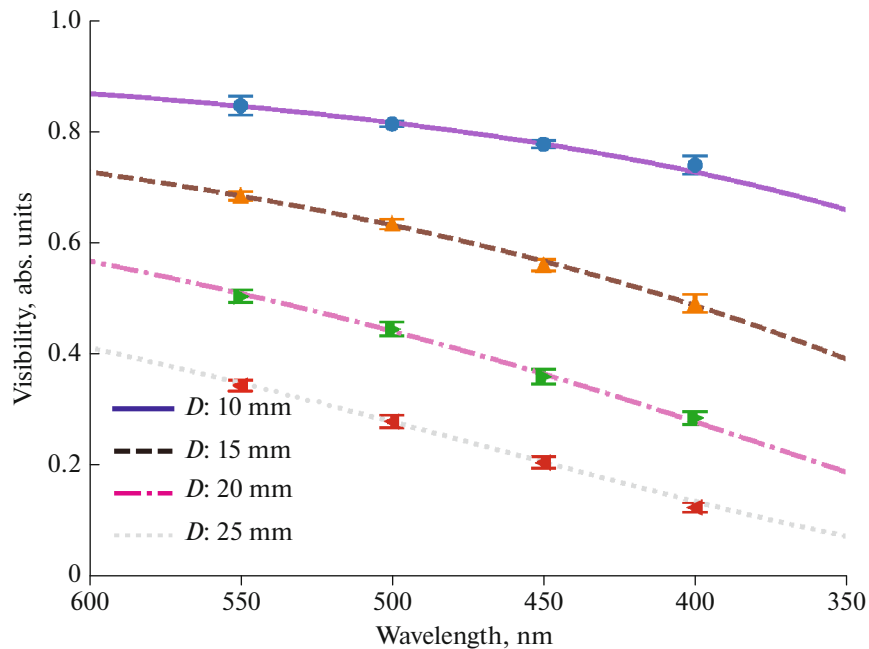

Fig 12. Dependences of visibility on the wavelength for different distances between the aperture slits.

sured variation in visibility as a function of spatial frequency ν of the interference pattern, which corresponds to the employed combinations of D and λ displayed in Fig. 12. Finally, Fig. 14 combines the values of the vertical size of the beam calculated using all the interferograms obtained. The accuracy of measurements was limited by the noise in the recorded interference pattern. It can be seen that the vertical dimensions of the beam obtained for various combinations of wavelengths and interslit distance D and λ are in good agreement. The total time of measurement was about 3 h, which is, however, much less than the

beam lifetime in the accelerator, which is 26 h, so the dependence of the vertical size on current can be neglected. The error in determining the leftmost point in the plot shown in Fig. 14 is determined by the behavior of the error function described by Eq. (4) and displayed in Fig. 2. Figure 15 shows the measured beam size as a function of the exposure time. The effect of vibrations is reduced by decreasing the exposure time to a value less that 2 ms; however, the decrease in the amount of light reasults in deteriorated signal/noise ratio and the accuracy of the determination of size. As a whole, the vertical beam size measured
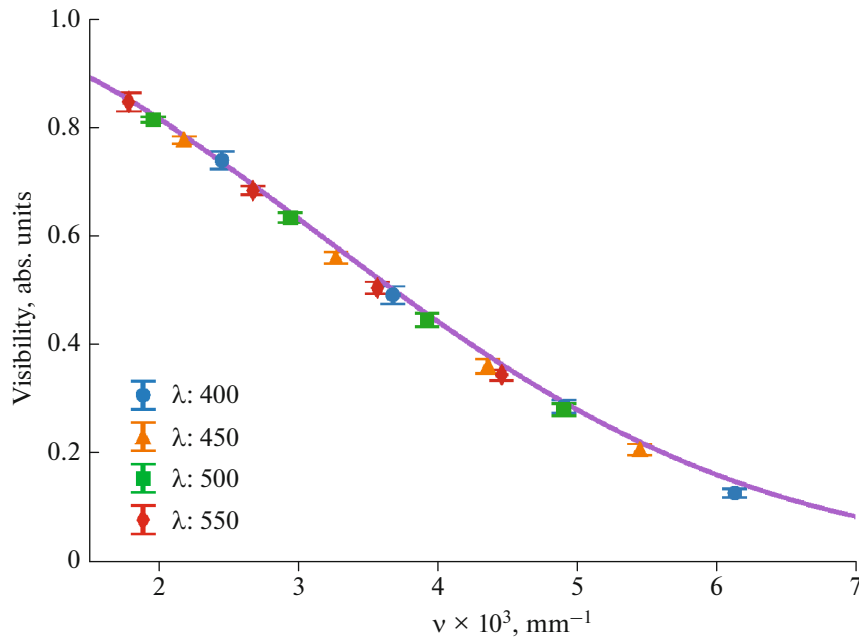
Fig 13. Visibility versus spatial frequency ν.
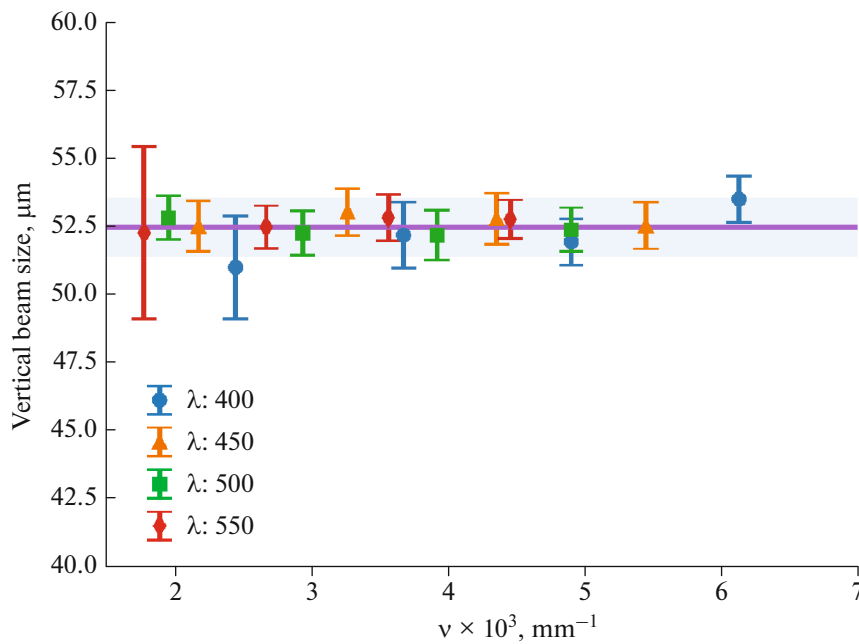

Fig 14. Dependence of the measured size on the spatial frequency ν.

in the experiment agrees well with the value determined two year earlier, which is an indicator of the operational stability of the OOS KSRS storage ring.

CONCLUSIONS

(1) The spectrum of low-frequency transverse beam oscillations in the KSRS has been measured. It is shown that vibrations with frequencies greater than 10 Hz increase the transverse size of the beam by 10–15%. The degree of influence of lower frequency oscillations on the apparent beam size requires additional study.

(2) The spectral method of scanning the visibility of the interference pattern for measuring the transverse dimensions of the beam has been experimentally tested.

(3) Generally speaking, the measured beam size can be affected both by dipole oscillations of its center of gravity caused by current pulsations of transverse
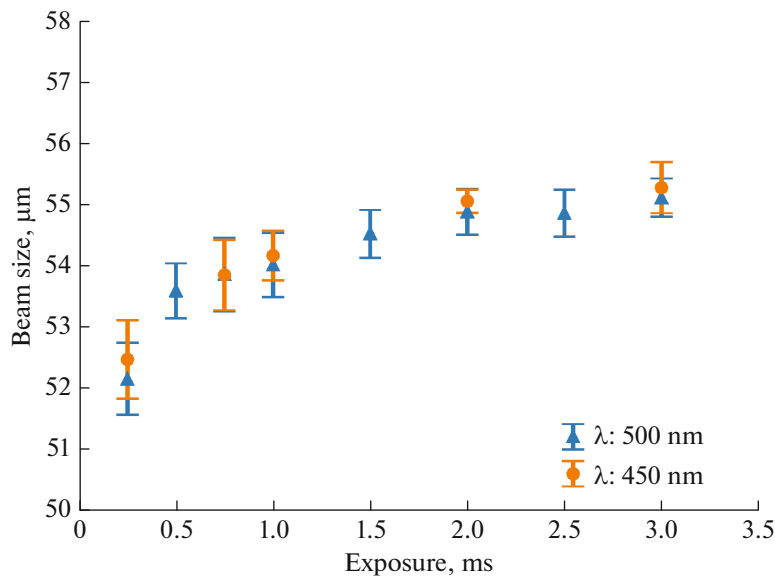
Fig 15. Dependence of the measured size on the exposure time of the recording camera.

correctors and bending magnets and by quadrupole oscillations associated with current pulsations in quadrupole lenses. One can try to detect quadrupole fluctuations in the beam size by analyzing changes in the visibility of the interference pattern, but at this stage we have limited ourselves to studying the spectrum of dipole fluctuations, responding to requests from the KSRS team.

CONFLICT OF INTEREST

The authors declare that they have no conflicts of interest.

REFERENCES

1. S. Shin, "New era of synchrotron radiation: fourth-generation storage ring," AAPPS Bull. **31**, 21 (2021). https://doi.org/10.1007/s43673-021-00021-4

2. N. Simos, "Synchrotron facilities: vibration and stability challenge," Synchrotron Radiat. News **32**, 2−3 (2019). https://doi.org/10.1080/08940886.2019.1654825

3. R. O. Hettel, "Beam stability at light sources," Rev. Sci. Instrum. **73**, 1396−1401 (2002). https://doi.org/10.1063/1.1435812

4. T. Mitsuhashi, "Beam profile and size measurement by SR interferometer," in *Proceedings of the Joint US-CERN-Japan-Russia School on Particle Accelerators, Montreux and CERN, Switzerland, 1998,* Ed. by S. I. Kurokawa, S. Y. Lee, E. Perevedentsev, and S. Turner (World Scientific, 1999) https://books.google.ru/books?id=BMWpKZOjzmMC.

5. T. Naito and T. Mitsuhashi, "Very small beam-size measurement by a reflective synchrotron radiation interferometer," Phys. Rev. Spec. Top.−Accel. Beams **9**, 122802 (2006). https://link.ap.org/doi/10.1103/PhysRevSTAB.9.122802.

6. O. Meshkov, V. Dorokhov, A. Stirin, V. Korchuganov, A. Khilchenko, et al., "A new station for optical observation of electron beam parameters at electron storage ring SIBERIA-2," J. Instrum. **11**, P12015−P12015 (2016). https://doi.org/10.10881748-02211112p12015

7. V. L. Dorokhov, Candidate's Dissertation in Engineering (Novosibirsk, 2021).

8. M. Blokhov, V. Leonov, E. Fomin, et al., "Kurchatov synchrotron radiation source facilities modernization," in *Proceedings of the 22nd Russian Particle Accelerator Conference RuPAC 2010.*